EFFECTS OF TROPOPAUSE AND POTENTIAL VORTICITY ANOMALY ON FRONTOGENESIS*

Hou Dingchen (侯定臣), *Gao Xuehao* (高学浩), *Zhuang Xiaolan* (庄小兰)

and *Zhang Yong* (张 勇)**

Nanjing Institute of Meteorology, Nanjing 210044

Received July 25, 1996; revised January 17, 1997

ABSTRACT

A two-dimensional, semi-geostrophic numerical model incorporating the tropopause and stratosphere is used to investigate the effects of a positive potential vorticity anomaly and latent heat release on the frontogenetic process and the structure of the resulting frontal zone. It is demonstrated that (1) the inclusion of tropopause and stratosphere significantly changes the frontal structure only in the upper levels; (2) a clearly defined quasi-equivalent barotropic structure and a region of upward motion of finite width appear when a positive potential vorticity anomaly exists on the warm side of the maximum baroclinity in the lower troposphere, especially when it is located on the south edge of the baroclinic zone; (3) the above mentioned structure deteriorates as the frontogenesis proceeds in a dry atmosphere but can be maintained in a moist frontogenetic process with condensational heating; (4) the combination of a positive potential vorticity anomaly and the latent heat release is able to accelerate the frontogenesis significantly with the time needed to form an intense frontal zone reduced to less than 15 h. The results have significant theoretical importance in understanding the complex nature of frontal structure and frontogenesis, especially in understanding the dynamic structure of the subtropical frontal zone observed during early summer over East Asia.

Key words: tropopause, potential vorticity anomaly, frontogenesis, equivalent barotropic structure, subtropical frontal zone-Meiyu front system

I. INTRODUCTION

Two-dimensional, semi-geostrophic frontogenetic model successfully simulated the principal features of surface fronts and their evolution and thus explained the formation and evolution of intense frontal zone, especially the polar fronts (e. g. Hoskins and Bretherton 1972; Thorpe and Emanuel 1985; Moore 1987). However, most of the previous studies of frontogenesis investigated a fluid of uniform potential vorticity or a fluid with potential vorticity variation in the vertical only. In addition, the evolution of the ageostrophic secondary circulation associated with the frontogenesis was emphasized without much attention on the frontal structure.

* This research is supported by the National Natural Science Foundation of China.

** Currently affiliated with Sichuan Province Meteorological Bureau.

Operational weather analysis and diagnostic studies suggest that the real structure of some atmospheric fronts is rather different from the above mentioned results of simulation. The Meiyu front, observed in early summer over East Asia, has some unique characteristics, as revealed from recent analyses (e. g. Hou 1992; Hou et al. 1996; Akiyama 1990). If the subtropical frontal zone-jet system in the upper troposphere and the weak Meiyu front in the lower troposphere are considered as one system, the corresponding axis of the maximum baroclinity can be seen throughout the whole troposphere with the baroclinity being rather weak or the slope of the axis being very flat at some level in the mid-lower troposphere. As a result, the structure of the Meiyu front has characteristic features in terms of other derived quantities: There is a region of positive relative vorticity of finite width with its axis nearly vertical and capped by a region of negative vorticity, forming a typical equivalent barotropic structure; The ascent associated with the frontogenesis is limited in a narrow zone, with rather high intensity; The slope of the axis of maximum baroclinity is sharp and the lower level frontal zone is frequently seen separated from its upper level counterpart. The analysis of potential vorticity (Hou 1991; Hou et al. 1996) showed that a region of relatively high potential vorticity always exists in the mid-lower troposphere during the period of Meiyu, with a high potential vorticity center formed in the troposphere. Figure 1 shows an example. This suggests that the structure of the subtropical frontal zone-Meiyu front system is closely related to the positive potential vorticity anomaly in the lower troposphere. On the other hand, precipitation is one of the main characteristics of the Meiyu weather and the effect of latent heat release on the structure of the frontal system can not be neglected. In addition, the frontal structure simulated without considering the stratosphere is quite different from the observation.

Based on the foregoing consideration, the classic two-dimensional semi-geostrophic frontogenetic model is modified by incorporating the stratosphere and tropopause, as well as a positive potential vorticity anomaly (PVA) in the lower troposphere and the parameterization of latent heat release. The emphasis is put on the effects of the tropopause and the positive PVA on the frontal structure and the frontogenetic process.

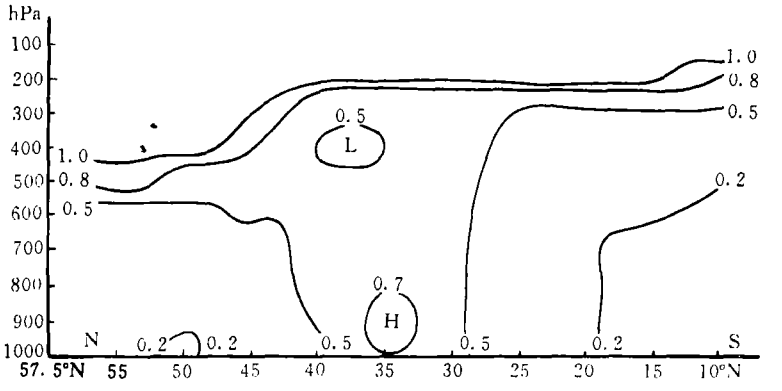

Fig. 1. Vertical cross section along 120°E averaged over the period May 21 — 25, 1991, showing contours of potential vorticity in unit of potential vorticity unit (PVU, 10^{-6} m^2 K kg^{-1} s^{-1}).

We aim to explore the mechanism of the formation of the equivalent barotropic structure of Meiyu front. However, we have to leave the consideration of the weakness of the baroclinity in the lower levels, another characteristics of Meiyu front, to another paper.

II. MODEL DESCRIPTION AND EXPERIMENT DESIGN

After Hoskins and Bretherton (1972), with the quasi-static and Boussinesq approximations, the two-dimensional, semi-geostrophic frontogenesis of a non-frictional atmosphere forced by a deformation flow incorporating diabatic heating is governed by the following set of equations:

$$\frac{\mathrm{d}\theta}{\mathrm{d}t} = S, \qquad \text{(for the top and bottom boundaries)} \tag{1}$$

$$\frac{\mathrm{d}q}{\mathrm{d}t} = q\left(\frac{\partial\theta}{\partial Z}\right)^{-1}\frac{\partial S}{\partial Z}, \tag{2}$$

$$\frac{\partial^2\Phi}{\partial X^2} + \frac{f^3\theta_0}{\rho g q}\frac{\partial^2\Phi}{\partial Z^2} = f^2, \tag{3}$$

$$\frac{\partial^2\Psi}{\partial Z^2} + \frac{\rho g}{f^3\theta_0}\frac{\partial}{\partial X}\left(q\frac{\partial\Psi}{\partial X}\right) = -2\frac{\alpha\rho}{f^2}\frac{\partial^2\Phi}{\partial X\partial Z} - \frac{g\rho}{f^3\theta_0}\frac{\partial S}{\partial X}, \tag{4}$$

$$W = -\frac{q}{f}\left(\frac{\partial\theta}{\partial Z}\right)^{-1}\frac{\partial\Psi}{\partial X}. \tag{5}$$

where

$$\frac{\mathrm{d}}{\mathrm{d}t} = \frac{\partial}{\partial t} - \alpha X\frac{\partial}{\partial X} + W\frac{\partial}{\partial Z}. \tag{6}$$

The above equations have been converted from physical space (x, y) to geostrophic momentum space $(X,Z) = (x + V_g/f, z)$, where V_g is the geostrophic wind along the frontal zone (in y direction). θ and q are potential temperature and potential vorticity, respectively; $\Phi = \varphi' + V_g^2/2$ is the modified gravitational potential, satisfying $fV_g = \partial\Phi/\partial X$; Ψ is the streamfunction of the cross-frontal ageostrophic vertical circulation, i.e. $\rho u_{ag} = \partial\Psi/\partial z$ and $\rho w = -\partial\Psi/\partial x$; the vertical velocity in the geostrophic momentum space is designated by W; $\rho = 1.225$ kg m^{-3}, $\alpha = 10^{-5}$ s^{-1} and $f = 10^{-4}$ s^{-1} is density, deformation coefficient and Coriolis parameter, respectively; S is diabatic heating rate and only latent heat release is considered in this study. S is specified as 0 in dry experiments, and parameterized in the moist experiment, following Thorpe and Emanuel (1985), by assuming that atmosphere is saturated and the equivalent potential vorticity q_e is small and positive, i.e.

$$S = (q - q_e) \times \frac{1}{2}\left(-\frac{\partial\Psi}{\partial X} + \left|\frac{\partial\Psi}{\partial X}\right|\right). \tag{7}$$

Equation (4) can be rewritten as follows:

$$\frac{\partial^2\Psi}{\partial Z^2} + \frac{\rho g}{f^3\theta_0}\frac{\partial}{\partial X}\left(q_a\frac{\partial\Psi}{\partial X}\right) = -2\frac{\alpha\rho}{f^2}\frac{\partial^2\Phi}{\partial X\partial Z}, \tag{4'}$$

where

$$q_a = \begin{cases} q_e, & \text{when } W > 0 \\ q, & \text{when } W \leqslant 0 \end{cases}$$

$q_e = 0.05$ PVU $= 0.05\times10^{-6}$ m^2 K kg^{-1}s^{-1} is assumed, as in Hou et al. (1994).

Given the initial potential vorticity field over the whole model domain and the initial

distribution of potential temperature at upper and lower boundaries, W can be diagnosed by solving Eqs. (3) and (4′) and using Eq. (5), and Eqs. (1) and (2) can be integrated to get θ and q distribution at later time. The integration is carried out in the geostrophic momentum space with a domain size of 5000 km × 15 km (10 km when no tropopause is used) and gridlengths of $\Delta X = 40$ km and $\Delta Z = 333$ m. Time step is taken as $\Delta t = 900$ s and the results are plotted in physical space.

In the experiment with uniform potential vorticity, the initial potential vorticity is taken as $q_0 = 0.267$ PVU. The experiments with tropopause are initialized by letting $q_0 = q^* + q'$, with

$$q^* = \rho^{-1}\left(\frac{\partial \theta}{\partial Z}\right) f\left[3.50 + 5.0\mathrm{tg}^{-1}\left(\frac{Z - Z_t}{1000.0}\right)/\pi\right], \tag{8}$$

where Z_t is the height (in m) of the tropopause, a function of X. $\partial\theta/\partial z = 3.274 \times 10^{-3}$ K m^{-1} the average value of the vertical gradient of θ in the troposphere. The initial PVA is expressed as

$$q' = \Delta q\left(1 + \cos\frac{\pi(X - X_0)}{L_m}\right)\left(1 + \cos\frac{\pi(Z - Z_0)}{H_m}\right)\delta, \tag{9}$$

where $\Delta q = 0.2$ PVU, $Z_0 = 2.5$ km, $H_m = 2.5$ km, $L_m = 800$ km, and δ is defined as

$$\delta = \begin{cases} 1, & \text{when } |X - X_0| \leqslant L_m \text{ and } |Z - Z_0| \leqslant H_m \\ 0. & \text{otherwise} \end{cases}$$

The upper boundary is taken as a constant θ surface and the lower boundary has its initial potential temperature distribution

$$\theta_b = \frac{2}{\pi}\Delta\theta + \mathrm{tg}^{-1}\left(\frac{X}{L}\right) + 293 \text{ K}, \tag{10}$$

where $\Delta\theta = 12$ K, $L = 350$ km, same as in Thorpe and Emanuel (1985).

The spatial dimensions H_m and L_m of the PVA in Eq. (9) are consistent with the observation that the horizontal and vertical scales of the anomaly are about 1000 km and 5 km, respectively. The center of the anomaly is taken as 2.5 km and its central intensity taken as 3 times of the background value, all similar to the results of diagnoses. The design of the experiments is mainly concerned with the existence and location of the potential vorticity anomaly. Hou et al. (1996) pointed out that the potential vorticity anomaly is located on the warmer side of the frontal zone, sometimes directly next to the baroclinic zone and sometimes farther inside the warm air mass. Therefore, X_0 is taken to be 400 km and 800 km to simulate the two circumstances. In this paper, the following experiments are compared:

EXP0: $q = q_0$ uniform PV, $S = 0$, Dry experiment;

EXP1: $q = q^*$ with tropopause, $S = 0$, Dry experiment;

EXP2: $q = q^* + q'$, $X_0 = 400$ km, PVA inside baroclinic zone, $S_0 = 0$, Dry experiment;

EXP3: $q = q^* + q'$, $X_0 = 800$ km, PVA inside warm air $S = 0$, Dry experiment;

EXPW: $q = q^* + q'$, $X_0 = 800$ km as EXP3, but $S \neq 0$, Moist experiment.

Among these experiments, EXP0 is the same as the uniform potential vorticity model of Hoskins (Thorpe and Emanuel 1985). EXP1 used to show the effects of tropopause, EXP2 and EXP3 used to investigate the influence of positive PVA, and EXPW employed to display the contribution from latent heat release.

III. THE EFFECTS OF TROPOPAUSE

The tropopause used in this study, is a thin layer of transition between the troposphere and the stratosphere, with the stratospheric value of potential vorticity being 5 times as great as the tropospheric value. It is also a transition layer from a lower value of static stability in the troposphere to the higher value in the stratosphere. To make the top of the model an isentropic surface, the troposphere is higher over the warmer region on the surface and lower over the colder region, and the horizontal gradient of potential temperature reverses near the tropopause.

In EXP0 (Thorpe and Emanuel 1985), $\partial\theta/\partial x$ and V_g, as well as some other derived quantities, have a symmetric distribution with the centers at upper and lower boundaries having same intensity. In EXP1, the experiment with a tropopause, however, this symmetric structure does not exist, although the distribution of quantities near the surface does not change significantly. The centers of various quantities in the upper half of the domain are significantly weaker, and becomes closed centers near the tropopause. Figure 2 is the initial distribution of the horizontal thermal gradient of EXP1, showing a uniform slope of the axis of the baroclinic zone, of about 1:70, similar to a typical polar frontal zone. Although some improvement is noticed, the positive vorticity is still limited in a thin layer directly above the surface, the same as in EXP0.

The vertical velocity in the stratosphere is much weaker than that in the troposphere. A pair of ascent and descent centers in the troposphere have their altitudes hardly changed, but shifted apart by about 400 km horizontally. This is consistent with the decrease in the baroclinity averaged over the whole model depth. It should be noted that the pair of centers are no longer symmetric in their intensity, with the ascent being slightly stronger. After 24 h of integration, the distribution of various quantities is roughly the same as at the initial time. However, as the baroclinity increases, the slope of the axis of the baroclinic zone decreases to some extent, and the central intensity of the

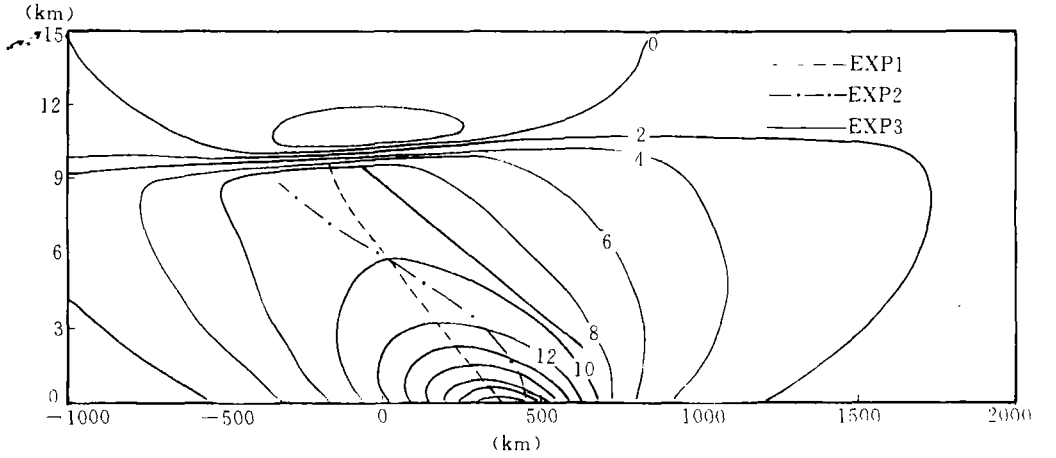

Fig. 2. Contours of $\partial\theta/\partial x$ (10^{-6} K m^{-1}) for $t=0$ in EXP1 with the axes of baroclinic zone for $t=0$ in EXP1, EXP2 and EXP3 depicted as heavy lines.

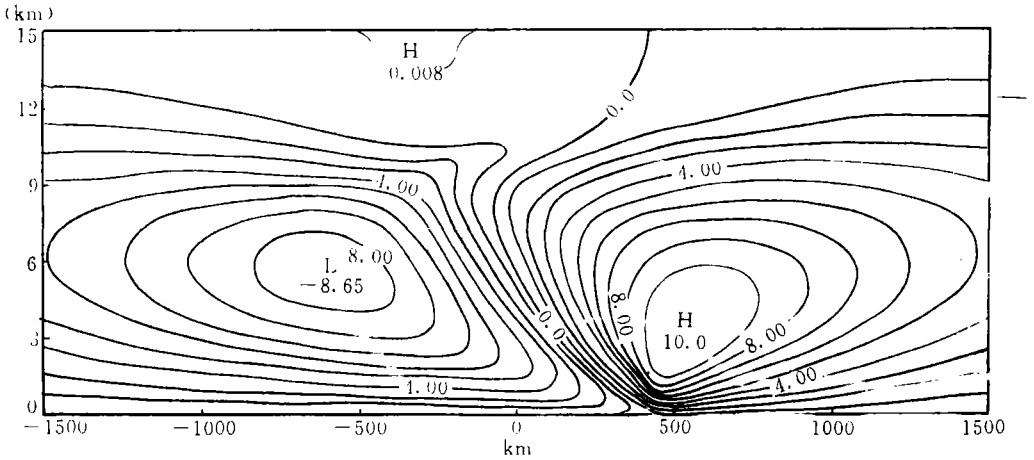

Fig. 3. Vertical velocity (10^{-3} m s^{-1}) for $t=24$ h in EXP1.

vertical velocity increases, although they are still less than 1.0 cm s^{-1} (see Fig. 3).

Generally speaking, the inclusion of the stratosphere and the tropopause modifies the frontal slope and makes it closer to the observed polar fronts and leads to a significantly stronger ascent center than the descent center. However, it has weak effect on the frontal zone in lower levels.

IV. THE EFFECTS OF POTENTIAL VORTICITY ANOMALY IN THE LOWER TROPOSPHERE

1. *The Initial Structure of the Frontal Zone*

The potential temperature field in the troposphere changes significantly with the inclusion of a positive PVA. As the region of a positive PVA is also a region of higher static stability (Hoskins et al. 1985), the isentropes in this region are relatively dense in the vertical direction. Figure 4 is the potential temperature field for $t=0$ in EXP2, with

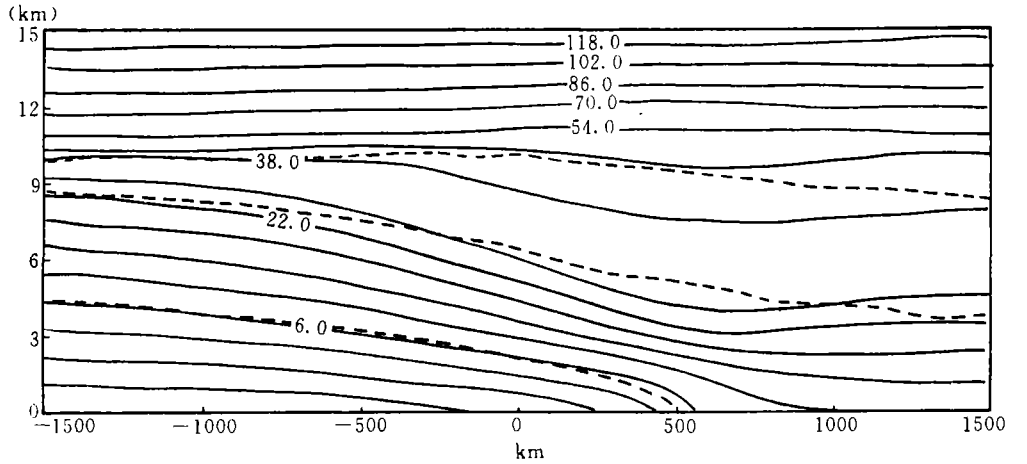

Fig. 4. Potential temperature (unit: K, a basic state of 293 K has been subtracted) for $t=0$ in EXP2. The heavy solid lines indicate some characteristic contours and the heavy dashed lines the same contours in EXP1.

some characteristic isentropes for $t = 0$ in EXP1 also depicted as heavy, dashed lines. Above 2.5 km height, the isentropes of EXP2 are curved downwards relative to EXP1, indicating warming as high as 8 K. Below that height, cooling is indicated. Therefore, the inclusion of a positive PVA implies a disturbance with colder air in the lower troposphere and warmer air in the mid-upper troposphere, and leads to a change in the location and the slope of the axis of the baroclinic zone. Compared with EXP1, the axis of the baroclinic zone in EXP2 shifts towards the warmer air in the lower layer and towards the colder air in the upper layer (Fig. 2) while the slope in the lower troposphere is increased. In addition, the horizontal potential temperature gradient in the troposphere increased, with the area enclosed by the 1 K (100 km)$^{-1}$ contour extending upwards to the tropopause (it reaches 6 km only in EXP1). When the positive PVA is located inside the warm air (EXP3), the frontal zone in the mid-upper layer also shifts towards warm side, and the axis of the baroclinic zone breaks two sections (Fig. 2). The lower level section has a very flat slope (1:160, similar to EXP0) while the upper level section has a slope of 1:100 and shifted towards the warm air by about 300 km. This is rather similar to the subtropical frontal zone over East Asia, which is separated from the surface polar fronts.

Figure 5 shows the absolute vorticity (ζ) distribution for $t = 0$ in EXP2 and EXP3.

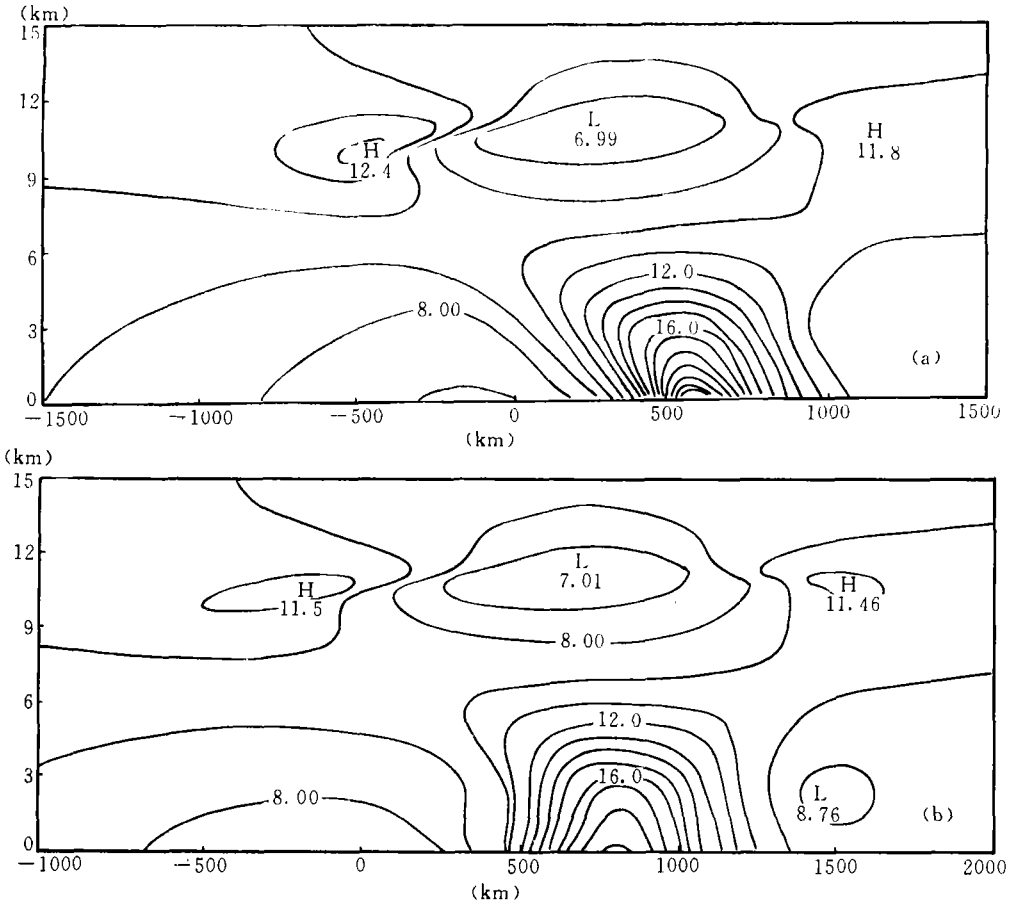

Fig. 5. Absolute vorticity distribution for $t = 0$ h in (a) EXP2 and (b) EXP3 (unit: 10^{-5} s^{-1}).

Compared with the case without anomaly (EXP1), the realm of significant positive relative vorticity ($\zeta > 10^{-4}\ s^{-1}$) is no longer limited in a thin layer near the surface but can be seen up to 5 km altitude. Furthermore, significant positive vorticity is concentrated in a narrow region in the horizontal direction. The intensity of high vorticity is increased from $1.44\times10^{-4}\ s^{-1}$ in EXP1 to $2.20\times10^{-4}\ s^{-1}$ (EXP2) and $1.94\times10^{-4}\ s^{-1}$ (EXP3). Negative vorticity is seen above the positive region to form a clearly defined equivalent barotropic structure. The slope of the positive vorticity region is sharp, being 1: 20 in EXP2 and virtually vertical in EXP3. In addition, the surface positive vorticity center is located to the warm side compared with EXP1 and EXP2, by about 250 km. It is separated from the region of maximum surface baroclinity and located to the south side of the upper level baroclinic zone. This is similar to the observation near a Meiyu front that the lower level positive vorticity center is associated with little thermal gradient.

By analyzing the vertical velocity fields for $t=0$ in the experiments EXP2 and EXP3 (not shown), it can be found that the positive PVA has the following effects on the frontogenetic secondary circulation: (1) the ascent center is located aloft the surface positive vorticity center, different from the experiment without PVA, where the ascent center is 200 km to the warm side of the surface vorticity center; (2) a zone of ascent of finite width is formed with descent motion appearing inside the warm air to the south of the disturbance; (3) the difference between the intensities of the ascent and descent increases with the ratio of ascent to descent exceeding 2.0; (4) the ascent and descent centers shift horizontally, towards the cold side in EXP2 and the warm side in EXP3; (5) the 0 contour of vertical velocity in the mid-upper layer shifts in the same sense as the ascent center. The results suggest that some principal features in the frontal structure of observed frontal zones, especially of the subtropical frontal zone observed over East Asia during early summer, such as the association of the ascent center with the surface positive vorticity center and the concentration of ascent flow and the rainfall in the horizontal direction, are related to the existence of the positive PVA in the lower troposphere.

Under the frontogenetic forcing of the deformation flow, the vertical velocity associated with the warm disturbance in the mid-upper layer and the cold disturbance in the lower layer (Fig. 4) is ascent and descent, respectively, near the PVA center. Overlaying this to the ascending flow to the warm side of the principal baroclinic zone, it is not difficult to explain the above mentioned intensification of the ascent and the shift of the 0 contour.

2. *Speed of Frontogenesis*

In a semi-geostrophic frontogenetic model, the intensity of positive vorticity in the lower troposphere increases exponentially and a discontinuity in momentum is expected as the absolute vorticity approaches infinity. In fact, the geostrophic momentum approximation and the semi-geostrophy approximation are no longer valid before the discontinuity is formed, due to the activity of small scale motion which tends to offset the frontogenetic effects of the deformation flow (Hoskins et al. 1984). Therefore, the integration of the model stops when the absolute vorticity exceeds 10 f, signifying the formation of an intense frontal zone. Figure 6 portrays the change of the intensity of the

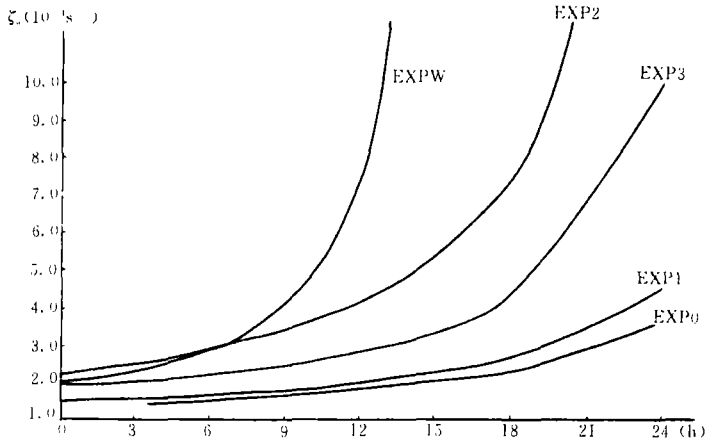

Fig. 6. The change of positive vorticity intensity with time, in various experiments.

surface high vorticity center in the lower troposphere in various experiments. It shows that (1) the incorporation of tropopause is in favor of the increase of lower level vorticity but an intense frontal zone is still not able to be formed in 24 h; (2) An intense frontal zone is formed in 24 h with the inclusion of a positive PVA and the time needed is only 20 h in EXP2; (3) The curves for EXP2 and EXP3 are coincident if the EXP2 curve is moved towards the right hand side, implying that the more rapid increase of vorticity in EXP2 is mainly due to its larger initial value, a result of the location of the high PVA with its induced positive vorticity being close to that induced by the baroclinic zone.

3. *Evolution of the Frontal Structure*

The frontal structure changes significantly as the frontogenetic process proceeds. In EXP3, the slope of the lower section of the axis of the baroclinic zone increases gradually

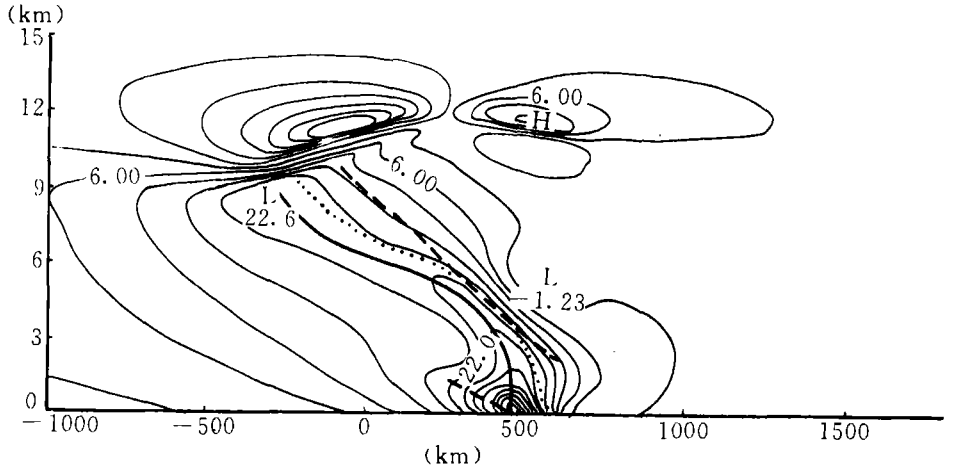

Fig. 7. The horizontal gradient of potential temperature (10^{-6} K m^{-1}) for $t=24$ h in EXP3. The heavy dashed line, heavy dotted line and the heavy solid line are the axis of the baroclinic zone at $t=0$, $t=12.5$ h and $t=24$ h, respectively.

and becomes nearly vertical at $t=12$ h. with the thermal gradient in the lowest 1.5 km layer evenly distributed in a belt 300 km wide. At $t=24$ h (Fig. 7), a narrow belt of intense baroclinic zone is formed with its axis rather sharp (1:40) below 3 km, but a much flatter slope in the upper troposphere. Between $t=12$ h to 24 h, the frontal zone moved towards the cold side by about 80 km. This feature of "warm front" has not been noticed in the previous studies. Similar changes also occur in EXP2.

The structure of the positive vorticity region in the lower troposphere also experiences significant changes. The slope of its axis in EXP1 does not change during the 24 h of integration but that in EXP2 and EXP3 decreases steadily, approaching 1:66 and 1:40, respectively. Even in EXP3, the equivalent barotropic structure is no longer clear. The width of the positive vorticity region is reduced to 300 km in 24 h.

At $t=24$ h, the ascent motion is no longer limited in a finite zone (Fig. 8), with the whole warm side occupied by ascent flow. The ratio of ascent to descent intensity is reduced from its initial value of 2.3 to 1.7 and 1.5 for EXP2 and EXP3, respectively. Inspecting the curves of temporal change of ascent intensity (not shown) reveals an increase first and then decrease in both EXP2 and EXP3. This is caused by the change of

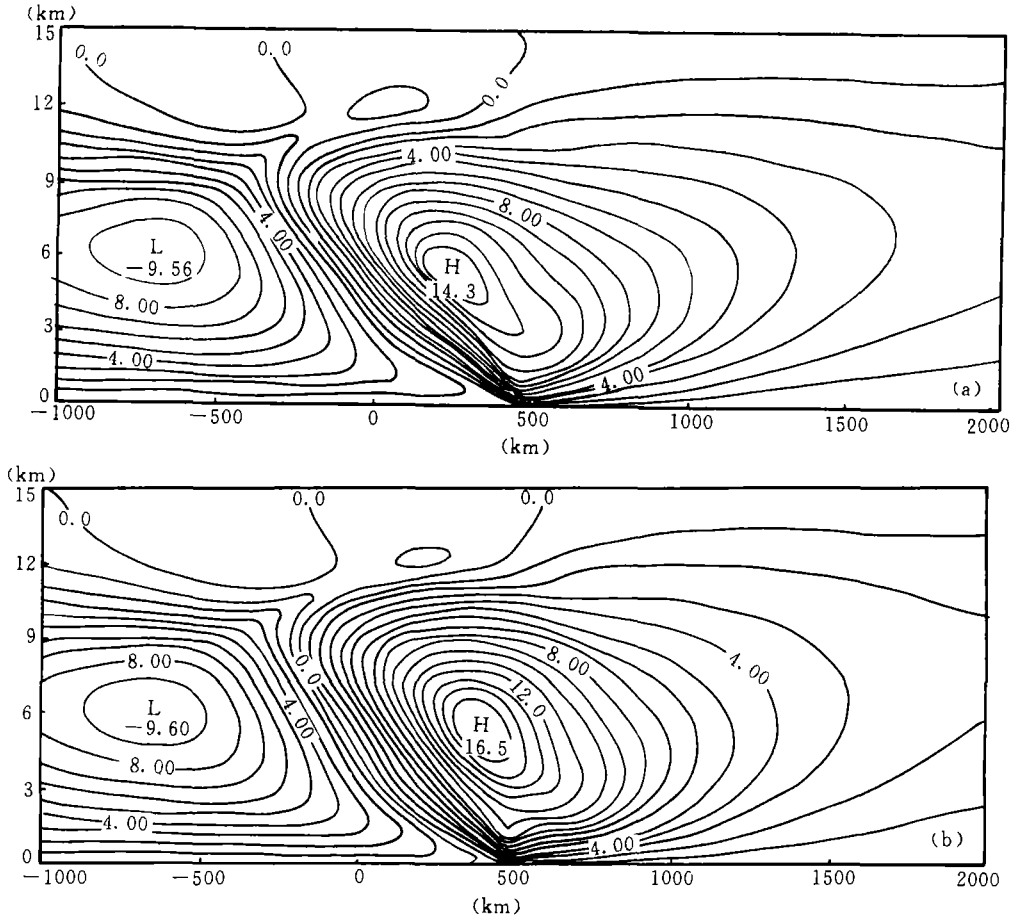

Fig. 8. Vertical velocity field for $t=24$ h in (a) EXP2 and (b) EXP3. The unit is 10^{-3} m s^{-1}.

the relative location of the ascent centers induced by the PVA and the large-scale baroclinity. Comparing the vertical velocity fields for $t=0$ and $t=24$ h tells us that the latter center moves by about 240 km, and the shift of the former center (Hoskins et al. 1984) is about $X_0(1-e^{-\alpha T})=230$ km, with the two roughly the same. However, because of the scale contraction of the PVA and the region of associated ascent, the phase difference between the two components of the vertical motion increases gradually in EXP2. The original overlaying of ascents is replaced by partial offsetting between ascent and descent, leading to the decrease of the resultant ascent center. In EXP3, the initial location of the PVA is to the warmer side of the ascent center induced by the large-scale baroclinity ($X_1=800$ km for the former and $X_2=700$ km for the latter) and shifts to its colder side at $t=24$ h ($X_1=330$ km and $X_2=470$ km), leading to a change in phase difference of decrease first and then increase, and a longer time period of ascents overlaying. Furthermore, at $t=24$ h, the ascent center is located at 300 km on the colder side of the surface vorticity center in EXP2 while the distance between the two is only 100 km in EXP3. The former is in favor of precipitation on the cold side while the latter is a favorable situation for stable and convective precipitation near the surface front and inside the warm air.

Summarizing the analyses of this section, one can find that the positive PVA near the lower troposphere has the effect of accelerating the frontogenesis. A positive PVA near the baroclinic zone is especially favorable for the formation of an intense front in a shorter period while the PVA inside the warm air is in favor of the formation and maintenance of a frontal structure similar to equivalent baroclinic structure. However, this equivalent barotropic structure becomes less clear later in both cases and the time needed for the formation of an intense frontal zone is still quite long.

V. THE EFFECTS OF LATENT HEAT RELEASE

The most important effect of the diabatic heating due to latent heat release, is to further accelerate the frontogenesis. From Fig. 6, it can be seen that EXPW, the experiment with the same initial condition as in EXP3 but incorporating latent heat release, produces an intense front 11 h in advance of EXP3. Compared with the moist experiment without positive PVA (Thorpe and Emanuel 1985), the formation of the intense front is also 10 h earlier. Therefore, the combination of positive PVA in the lower troposphere and the condensational heating is a favorable condition for an intense front to form in a short time period.

With the inclusion of latent heat release, the horizontal scale of the region of positive vorticity is further reduced. It is about 400 km at $t=13$ h, one third less than that in the dry experiment. The slope of its axis at this time is about 1: 20, consistent with the observed slope of Meiyu fronts.

The ageostrophic streamfunction for $t=14$ h in the moist experiment EXPW is shown in Fig. 9a. The ascent region of finite width is maintained and its width is further reduced to 500 km near the surface and 1000 km in the upper troposphere. This region is slantwise on the colder side and vertical on the warm side. The intense upward motion is concentrated in a narrow belt 200 km wide with its central intensity as high as 13 cm s^{-1},

an order of magnitude greater than the descent. The ageostrophic velocity (u_{ag}) field (not shown) shows a line of convergence with opposite (ageostrophic) wind vectors, sloping towards the colder side in the vicinity of the frontal zone in the lower troposphere; In the upper troposphere, a line of divergence is found. All of these were not found in the previous studies. With the condensational heating taken into consideration, the virtual static stability ($\partial\theta_v/\partial z$) in the ascent flow is much smaller than that in the dry cases ($\partial\theta/\partial z$) and much stronger vertical velocity is needed to offset the advection due to the deformation flow. This gives rise to the intense ascent flow and the strong convergence in the lower troposphere. From Fig. 9a it also can be seen that a part of the ascent flow ascends along the sloping frontal zone and another branch of it turns towards the warmer side in the upper layer to form a weak, but closed circulation cell. It is still a thermally direct circulation with the ascending air being warmer, similar to the monsoonal circulation cell observed over East Asia but much weaker.

Because the condensational heating occurs mainly in the vicinity of the positive PVA,

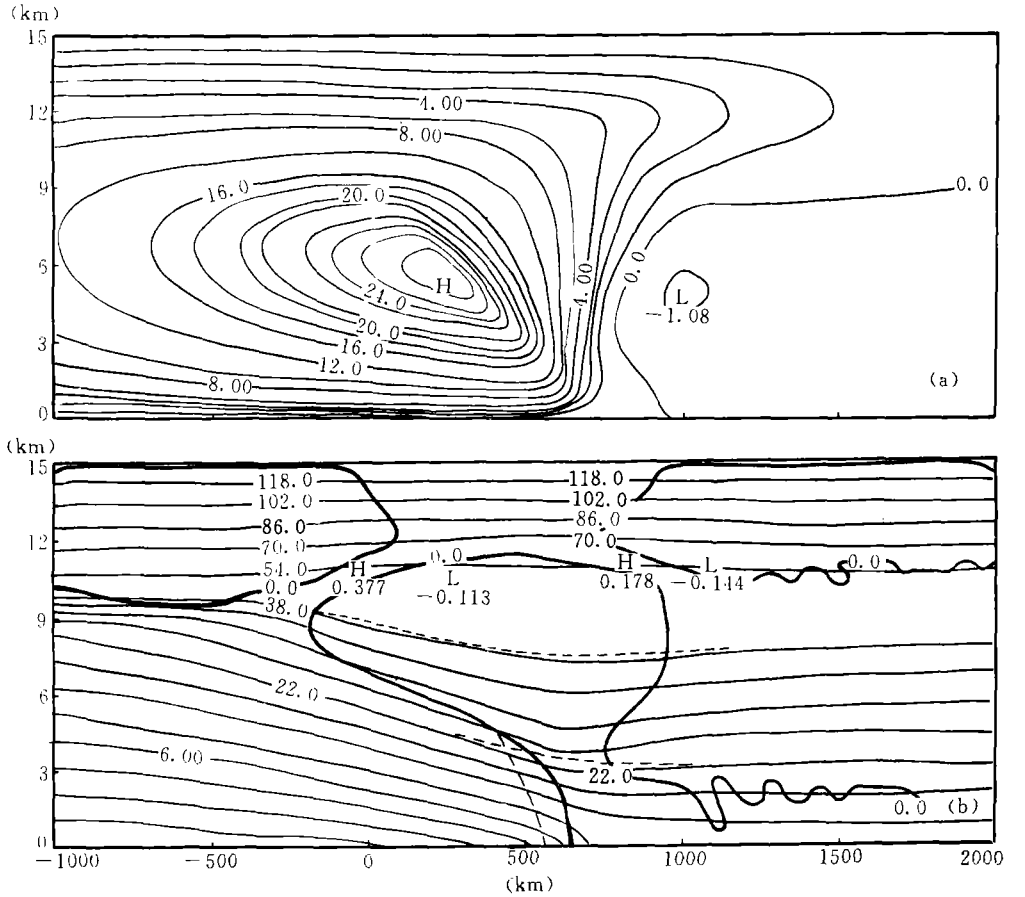

Fig. 9. (a) Ageostrophic streamfunction (10^3 m^{-1}s^{-1} kg) for $t=14$ h and (b) potential temperature (unit as in Fig. 4) for $t=12.5$ h in EXPW. In (b), the heavy solid line represents the axis of the baroclinic zone; The short and long dashed lines are the contour of potential temperature and the axis of the baroclinic zone, respectively same time but in EXP3.

it results in the intensification of the warm anomaly in the upper troposphere and the weakening of the colder anomaly in the lower troposphere, leading to the downward extension of the high PV anomaly. At $t=14$ h into the moist experiment EXPW, the positive PVA has a vertical configuration and a new center is found near the earth's surface (not shown), consistent with the results of Thorpe and Emanuel (1985). The effect of condensational heating on the thermal field is mainly increasing the baroclinity and change the orientation of the axis of the baroclinic zone. Figure 9b indicates that the axis of the maximum thermal gradient in the moist experiment EXPW is about 100 km to the warm side of its position in the dry experiment EXP3. Its location in the upper layer and its slope in the lowest 3 km remain unchanged. It should be noticed that a well-defined intense baroclinic zone has formed at $t=12.5$ h in the moist experiment, similar to the situation at $t=24$ h in EXP3.

In summary, the condensational heating has significant effects on the frontogenesis. It accelerates the frontogenesis and leads to the formation of an intense frontal zone in a period less than one day. It is also in favor of the formation and maintenance of the equivalent barotropic structure and a nearly vertical ascent flow in a narrow region and generation of large amount of rainfall.

VI. SUMMARY AND DISCUSSIONS

The analyses in this paper lead to the following conclusions:

(1) The inclusion of tropopause and the stratosphere has weak effect on the frontal structure in the lower troposphere and the speed of frontogenesis. However, it modifies the frontal structure and the slope of the frontal zone in the upper troposphere, making it closer to the observed structure of the polar frontal zone.

(2) The frontal structure in the troposphere can be significantly changed by inserting a positive PV anomaly on the warmer side of the lower tropospheric baroclinic zone. The changes include: ① the increase in the slope of the lower level frontal zone and its separation from the upper layer frontal zone; ② the upward extension of the region of positive vorticity into the troposphere and the formation of a quasi-barotropic structure with its axis of positive vorticity nearly vertical and capped by a region of negative vorticity; ③ the concentration of ascent flow into a region of finite width with its intensity significantly higher than the descent flow.

(3) The above mentioned characteristics are more clear when the positive PVA is inside the warm air. However, these features become weak as the frontogenesis proceeds in the dry atmosphere, no matter where the initial positive PVA is located.

(4) The condensational heating tends to maintain and intensify the above mentioned features and reduces the time needed for the formation of an intense frontal zone. Therefore, the combination of a positive PVA and the condensational heating is of primary importance in the formation of a frontal zone with an equivalent barotropic structure such as in the case of Meiyu front.

The positive PVA on the warm side of the baroclinic zone in the lower troposphere and the associated frontal structure discussed in this paper are generally consistent with the main features of the synoptic scale structure of the subtropical frontal zone over East

Asia during early summer. However, the surface thermal structure associated with Meiyu front is not well simulated, because of the adoption of surface potential temperature distribution used in the studies of classic polar fronts. Nevertheless, the results of this study still have significant theoretical importance. Firstly, the separation of the surface positive vorticity center and the surface baroclinity has been successfully simulated. If we take the Meiyu front in the lower troposphere as the vorticity center and the surface front at higher latitudes as the surface baroclinic zone, the simulation would have great similarity to the observation. Secondly, considering the heating effect at the earth's surface over the East Asia continent during early summer, the surface distribution of the potential temperature gradient would be quite different. Due to the large amount of surface heating, the principal baroclinic zone in the lower troposphere will retreat northward while the frontal zone in the upper troposphere remains at lower latitudes, leading to the separation of the lower level frontal zone from the upper level frontal zone. This is very similar to the Meiyu front with weak baroclinity in its vicinity but significant baroclinity to the north in the upper troposphere. In order to fully understand the subtropical frontal zone-Meiyu front system, it is necessary to employ a primitive equation model and a more realistic initial surface thermal condition.

REFERENCES

Akiyama, T. (1990). Large, synoptic and meso-scale variations of the Baiu front during July 1982. Part II. Frontal structure and disturbances, *J. Met. Soc. Japan*, **68**: 557—574.

Hoskins, B. J. and Bretherton, F. P. (1972). Atmospheric frontogenesis models: Mathematical formation and solution, *J. Atmos. Sci.*, **29**: 11—37.

Hoskins, B. J. et al. (1984). Formation of multiple fronts, *Quart. J. Roy. Met. Soc.*, **110**: 881—896.

Hoskins, B. J. et al. (1985). On the significance of isentropic potential vorticity maps, *Quart. J. Roy. Met. Soc.*, **111**: 877—946.

Hou Dingchen (1991). Potential vorticity structure of summer cyclones over the Changjiang-Huaihe valley, *Acta. Meteor. Sinica*, **5**: 40—50.

Hou Dingchen (1992). A comparative study on the structures of summer cyclones over the Changjiang-Huaihe valley, *Meteor. Science*, **12**: 93—99 (in Chinese).

Hou Dingchen, Gao Xuehao and Zhuang Xiaolan (1994). Numerical experiment on Pronto genesis near warm bump, *J. Nanjing Institute of Meteor.*, **17**: 276—283 (in Chinese).

Hou Dingchen, Zhuang Xiaolan and Ma Shengyu (1996). The Structure of subtropical rontal zone during the Meiyu period 1991, *J. Nanjing Institute of Meteor.*, **19**: 178—185 (in Chinese).

Moore, G. W. K. (1987). Frontogenesis in a continuously varying potential vorticity fluid, *J. Atmos. Sci.*, **44**: 761—770.

Thorpe, A. J. and Emanuel, K. A. (1985). Frontogenesis in the presence of small stability to slantwise convection, *J. Atmos. Sci.*, **42**: 1809—1824.